Separation Science and Technology
Publication details, including instructions for authors and subscription information:
http://www.informaworld.com/smpp/title~content=t713708471

Dehydration of Acetic Acid-Water Mixtures with Near Critical and Supercritical Fluid Solvents

M. A. Mccully[ab]; J. C. Mullins[a]; M. C. Thies[a]; I. J. Hartley[ac]
[a] Dept. of Chemical Engineering, Clemson University, Clemson, South Carolina [b] Sirrine Environmental Consultants Corp., Greenville, SC [c] Union Carbide Corp., North Seadrift, TX

To cite this Article Mccully, M. A. , Mullins, J. C. , Thies, M. C. and Hartley, I. J.(1988) 'Dehydration of Acetic Acid-Water Mixtures with Near Critical and Supercritical Fluid Solvents', Separation Science and Technology, 23: 12, 2065 — 2085
To link to this Article: DOI: 10.1080/01496398808075683
URL: http://dx.doi.org/10.1080/01496398808075683

SEPARATION SCIENCE AND TECHNOLOGY, 23(12&13), pp. 2065-2085, 1988

DEHYDRATION OF ACETIC ACID-WATER MIXTURES WITH NEAR CRITICAL AND SUPERCRITICAL FLUID SOLVENTS

M. A. McCully,* J. C. Mullins, M. C. Thies and I. J. Hartley†
Clemson University
Dept. of Chemical Engineering
Clemson, South Carolina 29634

ABSTRACT

Equilibrium tie lines and phase densities are presented for acetic acid-water mixtures with near critical propane at 361K and 52 bar. Experimental measurements were obtained with a static technique; the equilibrium phases were directly sampled with high-pressure liquid sample injection valves at the temperature and pressure of interest. The data obtained in this work indicate that near critical propane can be used to facilitate the production of glacial acetic acid from dilute acetic acid-water solutions. Both these experimental data and our earlier results for acetic acid-water mixtures with supercritical carbon dioxide have been used to test an equation of state which has recently been developed by Grenzheuser and Gmehling for systems which contain associating fluids. Results indicate that the equation's pure component parameters need to be refitted to represent the critical region more accurately.

INTRODUCTION

This paper is the second in a series concerning the separation of organic chemicals from aqueous mixtures by using near critical or supercritical (NC-SC) solvents. In an earlier paper, we presented equilibrium tie lines for the acetic acid-water-carbon dioxide system (1) at temperatures to 323 K and pressures to 139 bar.

*current address: Sirrine Environmental Consultants Corp., Greenville, SC 29606
†current address: Union Carbide Corp., North Seadrift, TX 77983

In this paper, liquid-liquid equilibrium compositions and phase densities are presented for acetic acid-water mixtures with NC liquid propane at 361 K and 52.0 bar. Propane is expected to be a superior solvent to carbon dioxide for the following reasons: (1) It forms a heterogeneous azeotrope of the first kind with water (2), which will allow one to significantly reduce the energy required to produce glacial acetic acid in a solvent recovery column. (2) Propane has a higher critical temperature. As a result, it can be maintained at liquid-like densities under moderate pressures at temperatures up to 373 K, which should increase the distribution of acetic acid in the solvent phase. To our knowledge, no experimental measurements for the acetic acid-water-propane system have previously been made.

In our earlier work, an equilibrium flow apparatus was used, and samples were collected both gravimetrically and volumetrically at ambient pressures. In this work, the apparatus has been modified for operation in a static mode, and high-pressure liquid sampling valves have been incorporated for direct sampling of the phases at equilibrium temperatures and pressures. These changes were made 1) because the corrections which must be made to the collected phases with a gravimetric/volumetric sampling technique are significant when propane is used and cannot be accurately calculated, and 2) to eliminate concerns regarding possible fluctuations in the feed pump flow rates, which would affect phase compositions. An additional advantage of the new technique is that phase densities are also obtained.

In order to design economical processes involving the use of NC-SC solvents, one needs to be able to represent the thermodynamic properties of the system. Recently, Grenzheuser and Gmehling (3) have developed a new equation of state which combines the "perturbed hard chain" theory with chemical theory. In this paper, we investigate the ability of this equation to predict our measured ternary phase behavior for acetic acid-water mixtures with both SC carbon dioxide and with liquid NC propane.

EXPERIMENTAL

Method

A schematic of the experimental apparatus is shown in Figure 1. Before an experimental run, the cell is charged with the components of interest. Two high-pressure liquid chromatography feed pumps (Milton Roy, model no. 396) are used to deliver the components as compressed liquids at a total constant flow rate ranging from 200 to 550 ml/hr. The inlet tubing to the propane pump is cooled with a water-ice mixture to ensure the delivery of a liquid. After leaving the pumps, the mixture enters a mixing/equilibrium coil, in which the two liquid phases are mixed together and heated to within 0.1 K of the view cell temperature. This coil consists of two 40-ft lengths of 1/16 in. o.d., 0.030 in. i.d. tubing interconnected by 9 ft of 1/8 in. o.d., 0.055 in. i.d. tubing. The equilibrated, two-phase mixture subsequently enters the view cell, which functions as a phase separator. After each phase has filled approximately one-half of the cell volume, the feed pumps are turned off, the valves are closed, and the contents of the cell are allowed to settle. Although our experience indicates that complete separation of the phases occurs within one hour, usually at least 3 hours are allowed.

The resulting equilibrium phases are sampled with Valco submicroliter HPLC injection valves (model no. 6CI4WHCI.E) at the equilibrium temperature and pressure. These sample valves have an internal sampling chamber volume of approximately 1 μl and are located in the lines leaving the top and bottom of the cell (see Figure 1). The dead volume between the cell and the sample valves is minimized with the use of 1/16 in. tubing with an i.d. of 0.010 in. To obtain a sample of either phase, the micrometering valve of interest is opened such that a liquid flow rate of about 1 μl/s through the sample valve is obtained. This flow is maintained for several seconds in order to completely flush the sample line. A sample is then injected into the gas chromatograph (GC) carrier gas stream by manually turning the sample valve from the "load" to the "inject" position. To ensure that the sample is completely vaporized after injection, the carrier gas tubing is preheated in the oil bath before entering the sample valve, and electric heating tape is wrapped around the carrier gas tubing from the oil bath to the GC injection port. During sampling, the pressure of the system is maintained constant with a 500 ml sample cylinder (Whitey model no. 304L-HDF4-500) which contains nitrogen at the system pressure. Diffusion of nitrogen from this pressure reservoir into the system is prevented by partially filling the reservoir with the acetic acid-water mixture of interest and by locating 10 ft of 1/8 in. o.d., 0.055 in. i.d. tubing between the reservoir and the mixing/equilibrium coil. Since samples were analyzed by GC, contamination by nitrogen could always be checked and was not observed.

The view cell is a liquid level gauge (Jerguson Co. model 11-T-20) with a modified cell body. The body was fabricated at Clemson University from a block of Carpenter 450 stainless steel. Its fluid chamber has been machined to the original height and depth but is reduced in width from 5/8 to 3/8 in. Stainless steel Belleville washers (Associated Spring Co.) are used on the cover plate bolts to compensate for thermal expansion effects and to ensure proper sealing at elevated temperatures. The maximum operating conditions of the cell are estimated to be 423 K and 250 bar. The internal volume of the cell is approximately 30 ml.

The mixing/equilibrium coil, the view cell, and the sample valves are immersed in a silicone oil bath. The bath temperature is controlled to within ± 0.01 K with a Yellow Springs Model 71A temperature controller and thermistor which are connected to a 750 watt heating element. Thermal gradients in the bath are less than 0.02 K.

Several safety features are included in the apparatus. A 3/8 in. polycarbonate shield surrounds the oil bath and protects the operator against a possible rupture of the view cell. A portable gas detector equipped with an alarm continuously monitors the apparatus for propane leaks. All effluent streams containing propane are vented from the building.

Materials

Propane with a stated minimum purity of 99.5% was obtained from Matheson Gas Products Co. Glacial acetic acid with stated purity of 99.8% was obtained from the Aldrich Chemical Co. These chemicals were analyzed with a Hewlett-Packard (HP) 5890A GC equipped with a flame ionization detector and a 530 μm x 5 m methyl silicone column. In both cases, impurity levels were less than 0.1%. Distilled water was used in the experiments.

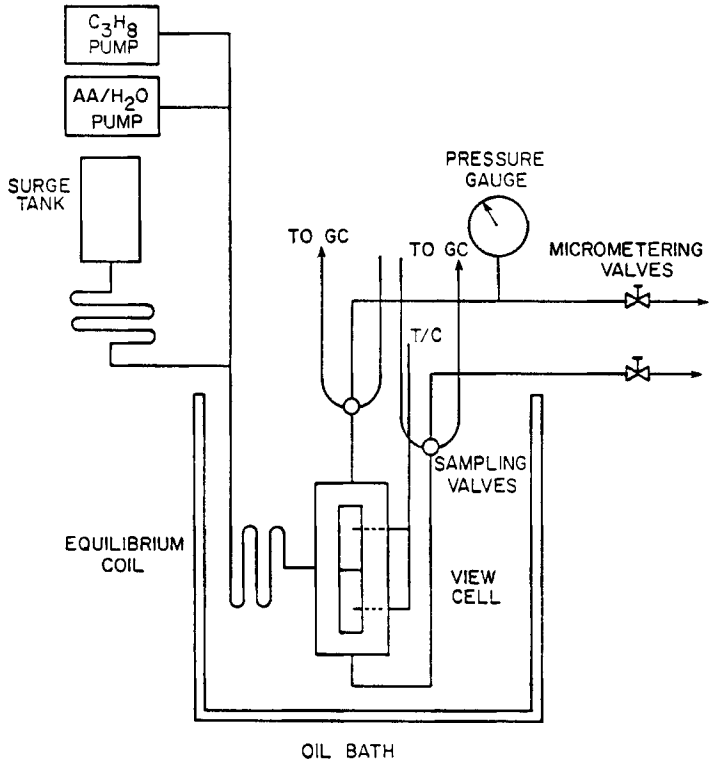

Fig. 1. Schematic of the Experimental Apparatus.

Measurements

The temperature of the two phases in the cell are measured with two type J thermocouples, which directly contact the fluid phases in the cell (Figure 1). Thermocouple voltage output is to a Keithley model 191 digital multimeter. The thermocouples and multimeter were calibrated as a unit to an accuracy of ± 0.05 K with a Rosemount 162CE platinum resistance temperature standard (RTD), a Leeds and Northrup (L&N) Mueller temperature bridge (model no. 8069-B), and an L&N dc null detector (model no. 9828). The calibration of the RTD is traceable to the National Bureau of Standards. Temperature gradients in the view cell as measured by the thermocouples were always found to be less than 0.1 K. The pressure in the view cell was measured with a Bourdon-tube type, 0-5000 psig Heise pressure gauge (model no. CC-87678). The pressure gauge was calibrated with a Budenberg dead weight pressure gauge tester (model no. 380H). Reported pressures are believed to be accurate to within ± 1 psi.

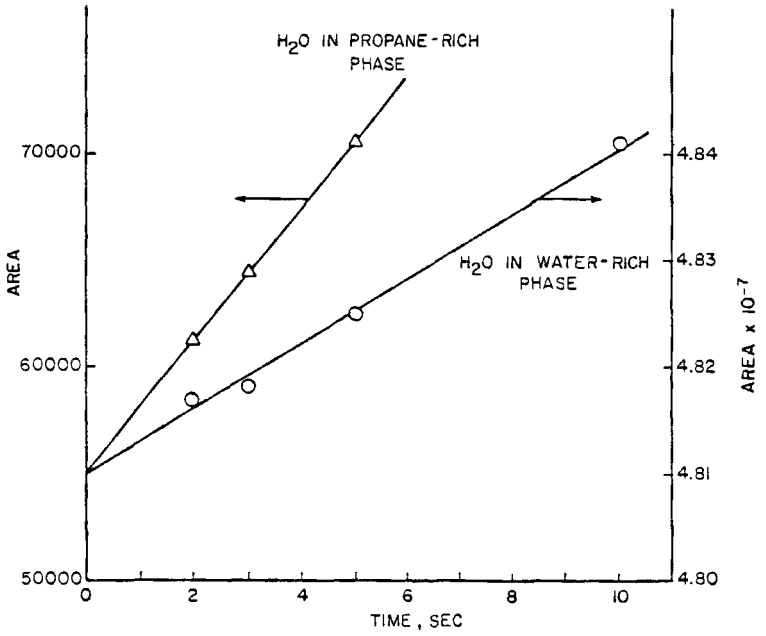

Fig. 2. Water Absorption in the Liquid Sample Valve vs. Load Time.

Samples were analyzed with an HP 5890A GC equipped with a thermal conductivity detector. Separation of the three components was achieved with a 6 ft x 2 mm i.d. glass column packed with Chromosorb 104, 80/100 mesh (Manville Corp.). The absolute mass of each component in a phase was determined by multiplying the GC area for that component by its response factor (i.e., mass/area ratio). From this information and a knowledge of the sample valve volumes, the overall composition and density of each phase was calculated.

The response factor for propane was determined by injecting propane-helium mixtures of known composition into the GC using a Valco gas sample valve (model no. CP3) with an external sampling loop of an accurately determined volume (0.9968 ml). The response factors for acetic acid and water were obtained by injecting liquid acetic acid-water mixtures of known composition and density into the GC with the liquid sample valves. The response of all 3 components was found to be linear to within $\pm 1\%$ over all concentration ranges of interest. The sample volumes of the liquid sample valves (1.03 and 1.22 µl) were obtained by injecting pure liquid propane of an accurately known density (4) and mass into the GC with these valves. To ensure that the response factors did not change, calibration samples were injected before each run. Details of the experimental technique are presented elsewhere (5).

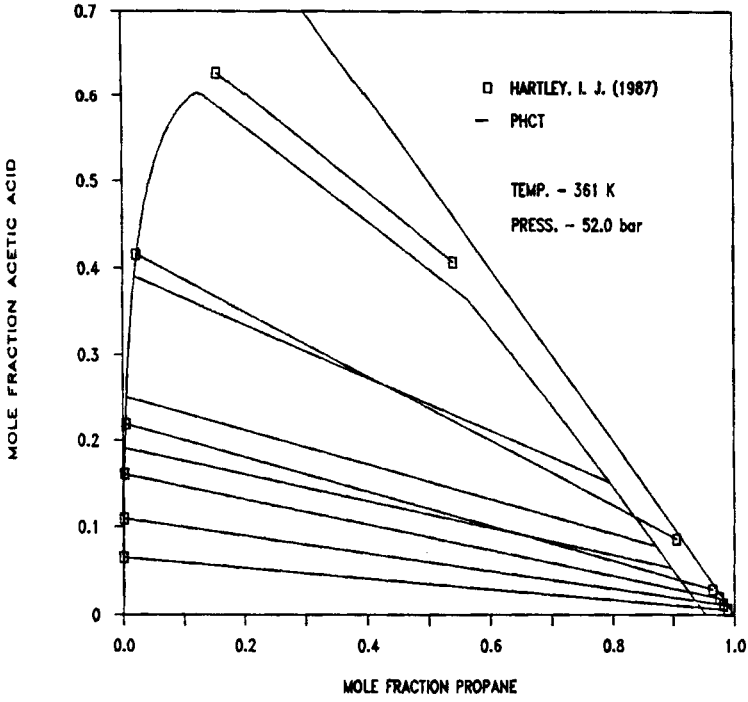

Fig. 3. Ternary Phase Diagram for Acetic Acid-Water-Propane System at 361 K and 52 bar.

Experimental Results

To verify that the apparatus was capable of producing good results, liquid-liquid equilibrium compositions were measured for the propane-water binary at 361 K and 52.0 bar for comparison with the work of Kobayashi and Katz (6). Our data agree with theirs to within 4 percent. Our results appear to be less accurate because of the absorption of water and propane into the polymer rotor of the liquid sample valve during sample loading. Since these components completely desorb when the sample is injected into the GC helium stream, higher than equilibrium values are obtained. To compensate for the absorption effect, all samples were injected at various sample valve "load" times; by linearly extrapolating to zero time, an estimate of the true phase composition was obtained. As seen in Figure 2, the uncertainty caused by this approximation was less than 1% of the measured value for the major components, but was about 5% for the minor components, which accounts for the difference between our results and those of Kobayashi and Katz. This absorption effect also occurred for the ternary system of interest; fortunately, the absorption of acetic acid was low enough that uncertainties in composition were less than 2% of the measured values at all concentrations.

Table I. Tie-Line Data for the System Acetic Acid-Water-Propane at 361 K and 52 Bar

Run #	Propane-Rich Phase			Water-Rich Phase		
	HOAC	H_2O	C_3H_8	HOAC	H_2O	C_3H_8
1	0.000	0.565	99.435	0.000	99.975	0.025
2	--	--	--	1.49	98.471	0.039
3	0.178	0.559	99.263	3.09	96.863	0.047
4*	0.548	0.562	98.890	6.55	93.368	0.082
5	1.14	0.580	98.280	10.98	88.855	0.165
6*	1.14	0.610	98.250	10.98	88.841	0.179
7	1.91	0.702	97.388	15.86	83.846	0.294
8*	1.87	0.638	97.492	16.07	83.669	0.261
9*	2.89	0.722	96.388	21.89	77.626	0.484
10*	8.56	0.916	90.524	41.84	55.97	2.19
11*	40.67	5.23	54.10	63.90	20.27	15.83

Note: The data are expressed in mole percent.
* Shown in Figure 3.

Liquid-liquid equilibrium compositions are presented for the acetic acid-water-propane system at 361 K and 52.0 bar in Figure 3 and Table I (The predictions of the equation of state are also shown on the figures and are discussed later). Due to the absorption effect discussed above, the accuracy of the reported compositions are dependent on the component and its concentration in a phase. At levels below 1 mole %, the propane and water compositions are believed to be accurate to $\pm 5\%$, at levels above 1 mole %, to $\pm 1\%$. The acetic acid compositions are believed to be accurate to $\pm 2\%$ at all concentrations.

Selectivities and distribution coefficients were calculated according to the following expressions:

$$\beta = \frac{\left[\frac{\text{mole fraction acetic acid}}{\text{mole fraction water}}\right]_{\text{solvent-rich phase}}}{\left[\frac{\text{mole fraction acetic acid}}{\text{mole fraction water}}\right]_{\text{water-rich phase}}} \tag{1}$$

$$\text{D. C.} = \frac{\left[\text{mole fraction acetic acid in solvent-rich phase}\right]}{\left[\text{mole fraction acetic acid in water-rich phase}\right]} \tag{2}$$

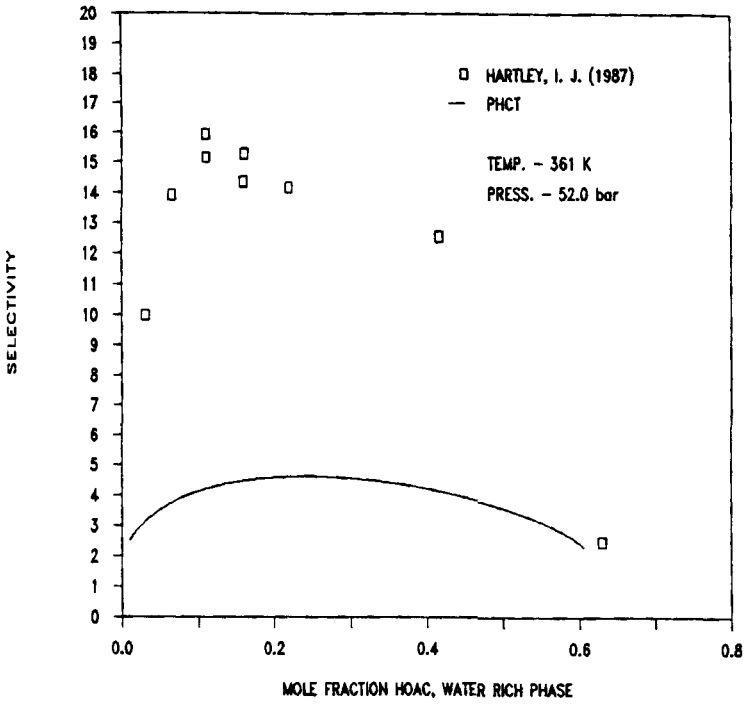

Fig. 4. Selectivity of Propane for Acetic Acid vs. Mole Fraction of Acetic Acid in the Aqueous Phase.

As shown in Figure 4, the experimental selectivities are relatively constant over a wide range of concentrations, approach one near the plait point, and drop dramatically at concentrations in the aqueous phase below 10 mole %. This drop at low concentrations is due to the increasing presence of acetic acid molecules in the monomer form, which are more difficult to extract than dimers. Distribution coefficients are shown in Figure 5.

Phase densities were also measured and are shown in Figure 6 and in Table II. Results are believed to be accurate to $\pm$ 1%, since the uncertainties in the minor component compositions have a negligible effect. Note how the density of the propane-rich phase decreases at low acetic acid concentrations. An explanation for the behavior is that the predominant acetic acid species are monomers at low concentrations, and they would be expected to have a very large partial molar volume in nonpolar propane. At higher concentrations, the nonpolar dimer form of acetic acid dominates, and the density of the propane-rich phase increases.

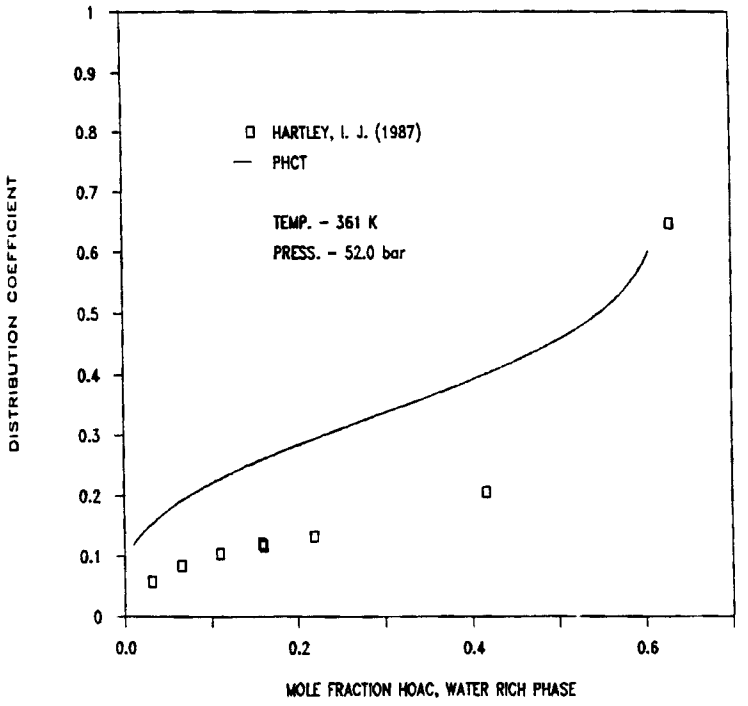

Fig. 5. Distribution Coefficient for Acetic Acid in Propane and Water vs. Mole Fraction of Acetic Acid in the Aqueous Phase.

Discussion of Experimental Results

As was previously mentioned, one of the reasons we chose to investigate propane as an extractive solvent was because of its ability to entrain water. For illustrative purposes, assume that one operated a solvent recovery column at 25 bar. At this pressure, the propane-water binary azeotrope consists of 99 mole percent propane (6). The data obtained in this work indicate that for acetic acid concentrations in the water-rich phase up to approximately 40 mole percent (see Run No. 10, Table I), the extract stream consists of greater than 99 mole percent propane on an acetic acid-free basis. Therefore, as long as the composition of the extract stream falls below that of the tie-line obtained in run no. 10, the solvent recovery column would produce glacial acetic acid as a bottom product and the propane-water azeotrope as the distillate from this stream. This final dehydration step would be a difficult separation if carbon dioxide was used as the solvent, since it does not entrain water.

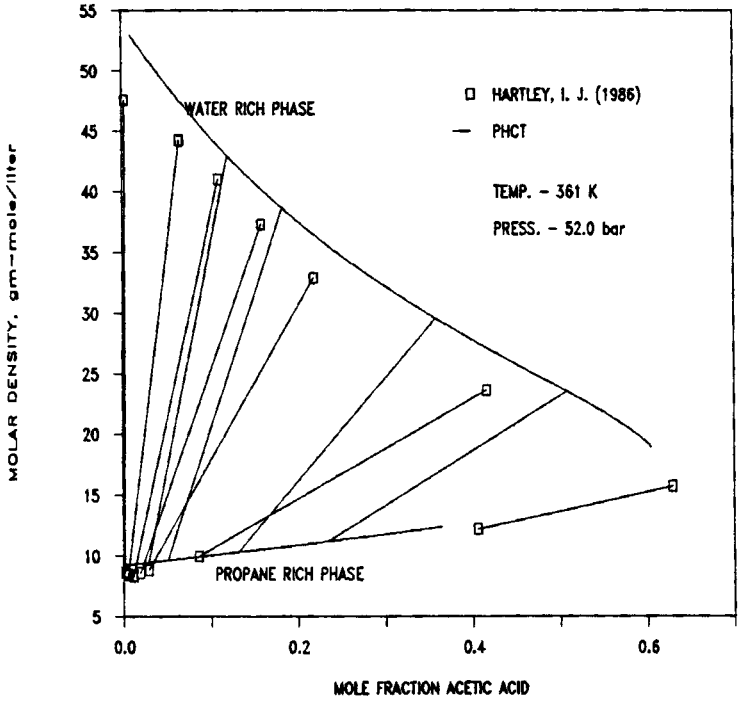

Fig. 6. Densities of Propane-Rich and Water-Rich Phases for Acetic Acid-Water-Propane System at 361 K and 52 bar.

Table II. Molar Densities of the Water-Rich and Propane-Rich Phases for the System Acetic Acid-Water-Propane at 361 K and 52 bar

Run #	Density of Water-Rich Phase (gmole/liter)	Density of Propane-Rich Phase (gmole/liter)	HOAC Mole Percent in Water-Rich Phase
1	50.3	8.65	0.00
2	49.0	--	1.49
3	47.5	8.66	3.09
4	44.2	8.46	6.55
5	41.0	8.37	10.98
6	41.0	8.31	10.98
7	37.3	8.60	15.86
8	37.0	8.66	16.07
9	32.9	8.86	21.89
10	23.6	9.98	41.84
11	15.7	12.15	63.90

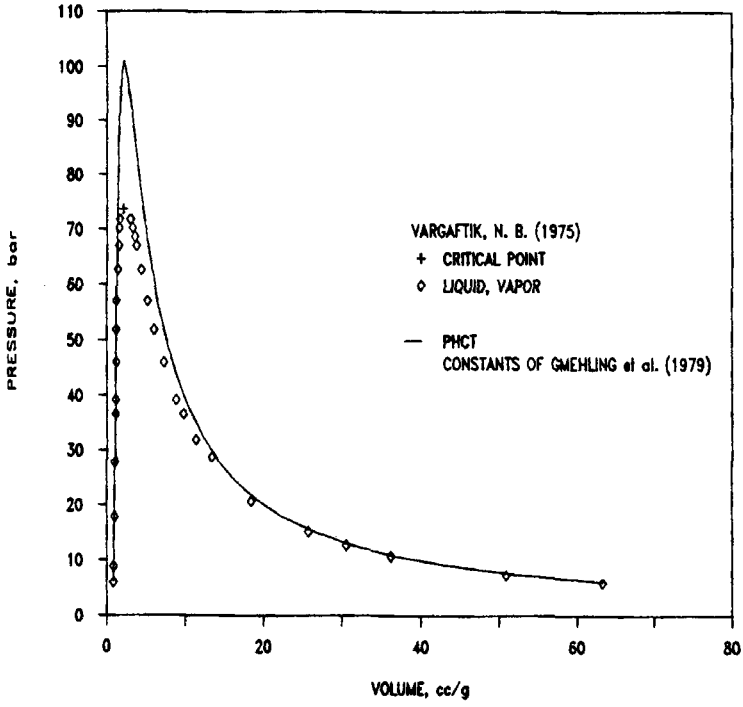

Fig. 7. Liquid and Vapor Saturation Curves for Carbon Dioxide.

Unfortunately, the equilibrium data indicate that propane is not superior to carbon dioxide in the actual extraction process. Comparing Figures 4 and 5 to 11 and 12, we see that neither the selectivities nor distribution coefficients for propane are substantially better than for carbon dioxide in the dilute acetic acid range. In conclusion, propane would be preferable to carbon dioxide as a supercritical solvent for producing glacial acetic acid; however, at 361 K and 52 bar, the selectivities and distribution coefficients are probably still too low for an economical process.

EQUATION OF STATE

Pure Components

The equation of state used in this work is described by Grenzheuser and Gmehling (3) and is an extension of the equation of Gmehling *et al.* (7). The equation is of the van der Waals type in which the pressure can be represented as the sum of an attractive and repulsive term:

$$P = P_{REPULSIVE} + P_{ATTRACTIVE} \quad (3)$$

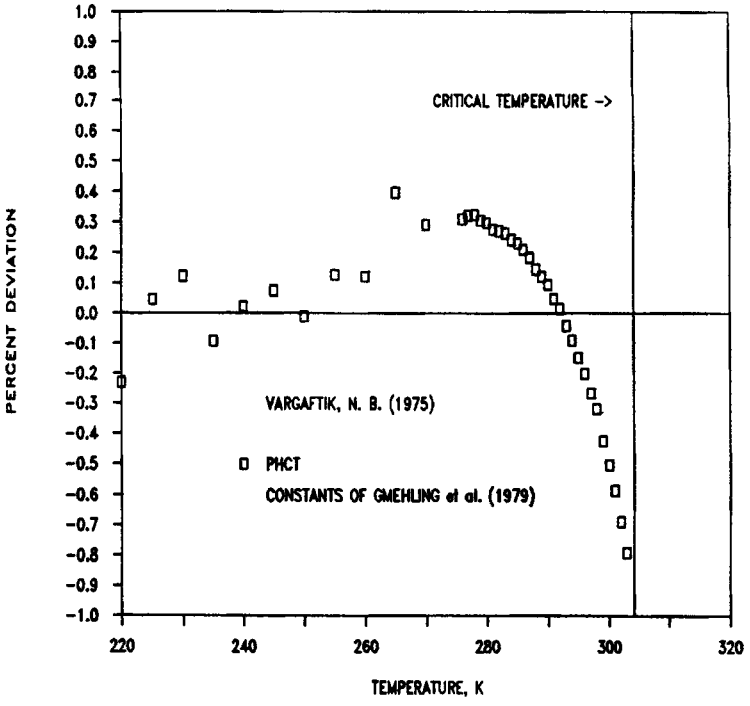

Fig. 8. Vapor Pressure Deviation vs. Temperature for Carbon Dioxide.

The repulsive and attractive terms are written in the same form as used by Donohue and Prausnitz (8) for the "perturbed hard chain" theory (PHCT) in which the repulsive term is expressed by the Carnahan-Starling relation (9) and the attractive term is based on the perturbation expansion of Barker and Henderson (10). For a pure substance

$$P = \frac{RT}{v}\left[1 + c\,\frac{4\xi - 2\xi^2}{(1-\xi)^3} + c\sum_{n}^{2}\sum_{m}^{5}\frac{m\,A_{nm}}{\tilde{T}^{n}\tilde{v}^{m}}\right] \qquad (4)$$

where

$$\xi = \frac{\pi\sqrt{2}}{6}\frac{v^*}{v}\,,\quad \tilde{T} = \frac{T}{T^*} = \frac{ckT}{\varepsilon q}\,,\quad \varepsilon = 105\ k\ ,\ \text{and}\ \tilde{v} = \frac{v}{v^*} = \frac{v\sqrt{2}}{N_A r\sigma^3}.$$

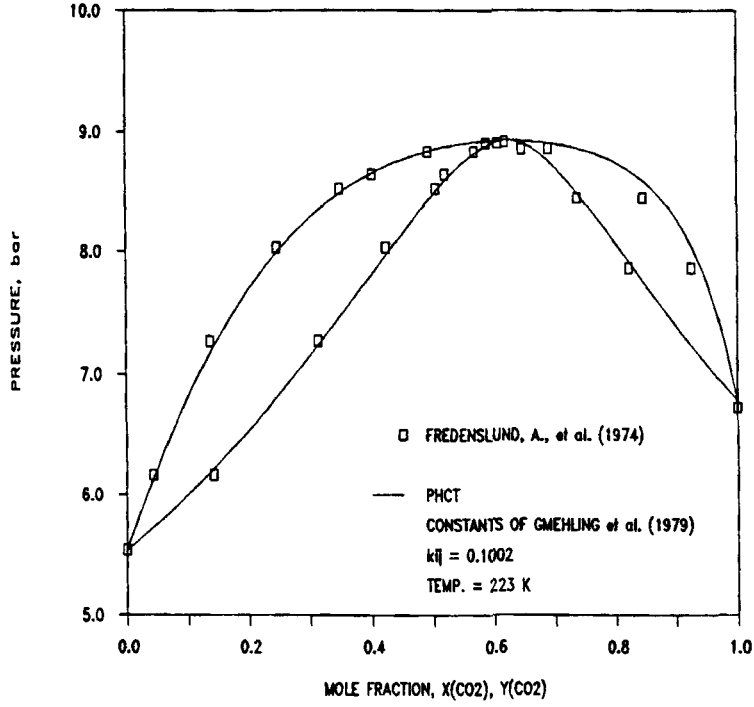

Fig. 9. Pressure vs. Composition Diagram for Carbon Dioxide-Ethane System at 223 K.

The PHCT equation contains the Prigogine parameter, c, which treats rotational and vibrational contributions in the partition function as equivalent external degrees of freedom. Thus for spherical molecules c=1 and for nonspherical molecules c>1.0.

T* is a characteristic energy parameter, v* is a characteristic size parameter, ε is the potential energy per unit surface area, q is the surface area per molecule, r is the number of segments per molecule, and σ is the hard core diameter per segment. The Boltzmann constant is designated by k. Donohue (11) chose ε/k equal to 105 K. Errors in ε are absorbed by the adjustable parameter q. $\tilde{T}$ is the reduced temperature. The reduced volume, $\tilde{v}$, is calculated by dividing the molar volume, v, by the hard-core molar volume v*. The reduced density, ξ, is the inverse of the reduced volume corrected for hexagonal packing.

For polar or associating compounds, Grenzheuser and Gmehling (3) adapted chemical theory to the PHCT equation. This theory assumes that the monomers can

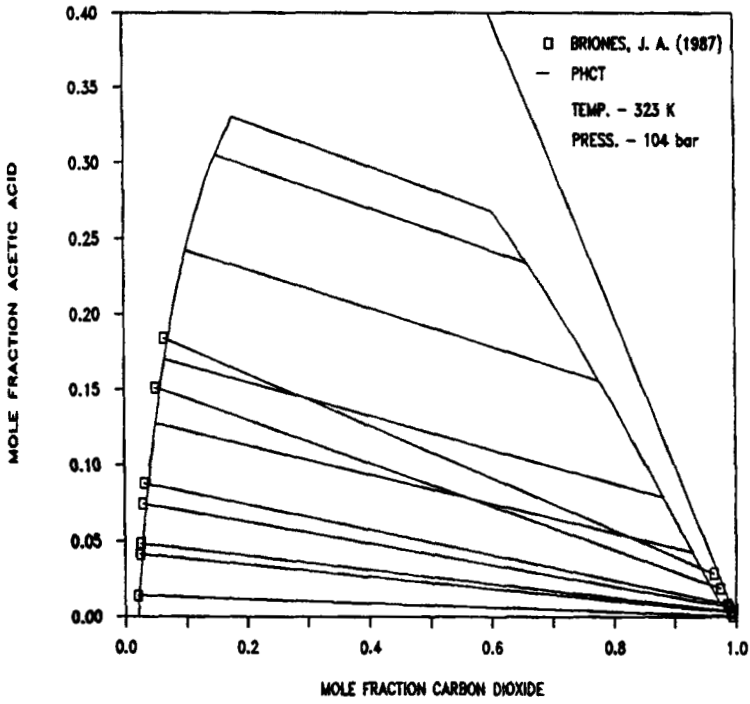

Fig. 10. Ternary Phase Diagram for Acetic Acid-Water-Carbon Dioxide System at 323 K and 104 bar.

associate to form dimers and oligomers such as

$$m_i + m_j \leftrightarrow d_{ij}$$
$$d_{ij} + m_k \leftrightarrow t_{ijk} \,. \tag{5}$$

For simplicity, only dimers and monomers were considered by Gmehling *et al.* (7). In the case of carboxylic acids this is ususally considered adequate, but for water, alcohols and other components this is clearly an averaging technique to prevent the calculations from being overly complex. For the formation of dimers the equilibrium constant is written in terms of the fugacity $\hat{f}_i$, the fugacity coefficient $\hat{\phi}_i$, the true mole fractions z_i, and the pressure P:

$$K_{ij} = \frac{\hat{f}_{ij}}{\hat{f}_i \hat{f}_j} = \frac{z_{ij}\hat{\phi}_{ij}}{z_i z_j \hat{\phi}_i \hat{\phi}_j P} \,. \tag{6}$$

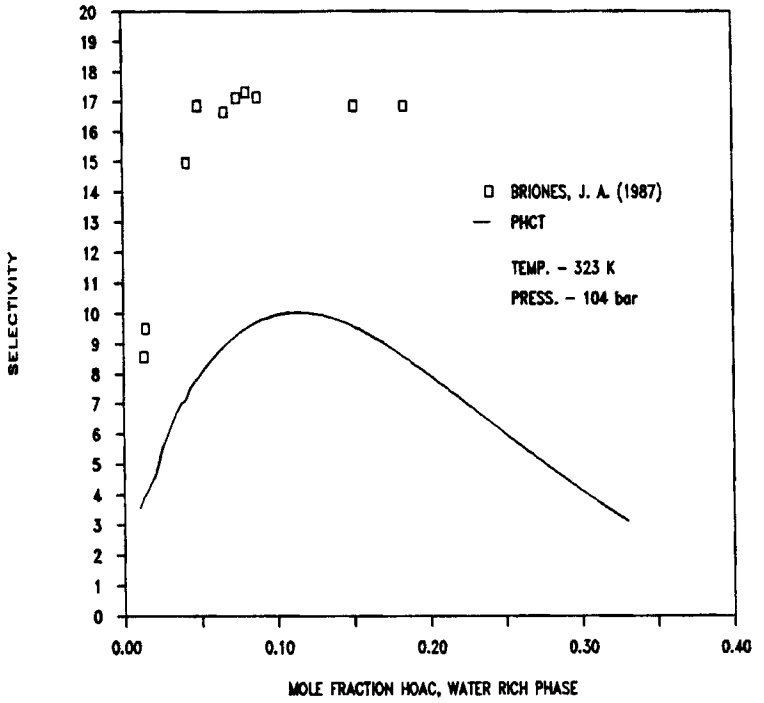

Fig. 11. Selectivity of Carbon Dioxide for Acetic Acid vs. Mole Fraction of Acetic Acid in Aqueous Phase.

The equilibrium constant K_{ij} is related to the standard free energy of reaction by

$$- RT \ln K_{ij} = \Delta g^{\circ}_{R} = \Delta h^{\circ}_{R}(T) - T \Delta s^{\circ}_{R}(T) \qquad (7)$$

For many applications Grenzheuser and Gmehling (3) found that Δh°_{R} and Δs°_{R} could be considered independent of T, but not for carboxylic acids. In general K_{ij} is given by

$$\ln K_{ij} = \frac{HO_{ij}}{T} + SO_{ij} + CO_{ij} \ln (T). \qquad (8)$$

For pure associating components this leads to six independent parameters: T^*, v^*, c, HO_{ii}, SO_{ii}, and CO_{ii}. For the dimers, $q_{ii} = 1.75qi$, $v^*_{ii} = 1.75v^*_i$, and $c_{ii} = 1.3c_i$. ε/k was assumed to be 105 K for the interaction of dimers as well as for monomers.

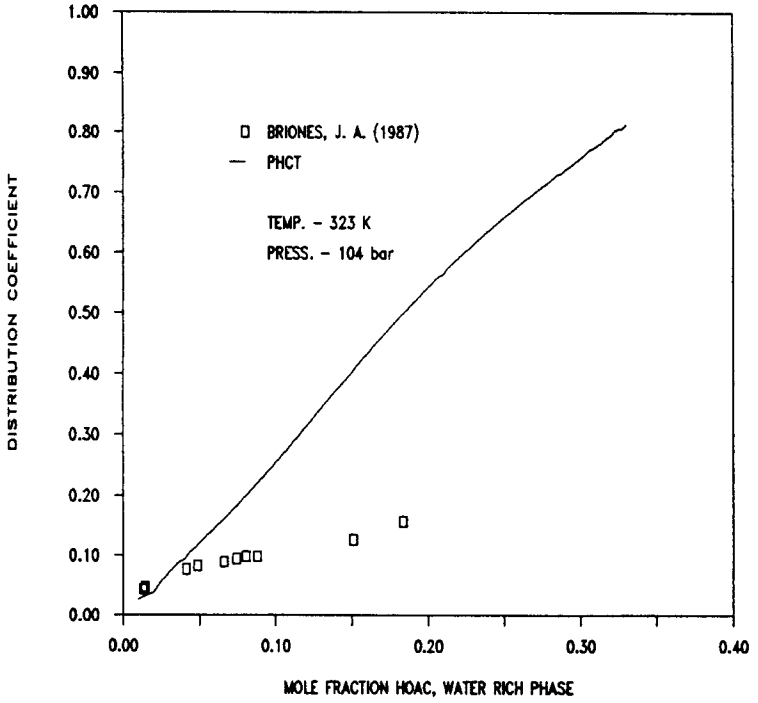

Fig. 12. Distribution Coefficient for Acetic Acid in Carbon Dioxide and Water vs. Mole Fraction of Acetic Acid in Aqueous Phase.

Mixtures

Only one additional parameter is used to fit the data for mixtures. The binary interaction parameter k_{ij} is defined by

$$\varepsilon_{ij}/k = 105\,(1 - k_{ij}). \tag{9}$$

The mixing rules for the cross dimers are given by

$$q_{ij} = 1.75\,(q_i + q_j)/2 \tag{10}$$

$$v^*_{ij} = 1.75\,(v^*_i + v^*_j)/2 \tag{11}$$

$$c_{ij} = 1.3\,(c_i + c_j)/2. \tag{12}$$

For the determination of the equilibrium constant, K_{ij}, for the cross dimers

$$HO_{ij} = (HO_i + HO_j)/2 \tag{13}$$

$$SO_{ij} = (SO_i + SO_j)/2 + ln\,2 \tag{14}$$

$$CO_{ij} = (CO_i + CO_j)/2. \tag{15}$$

For all strongly dimerizing systems SO_{ij} is treated as an independent parameter. For the interaction between two dimers, d_{ij} and d_{kl}, the interaction energy is given by

$$\varepsilon_{ij,kl} = (\varepsilon_{ik}\,\varepsilon_{il}\,\varepsilon_{jk}\,\varepsilon_{jl})^{0.25}. \tag{16}$$

Interaction energies between a monomer and its dimer have been set equal to those between the pure dimer of the monomer and the second dimer. The final expressions for calculating the mixture parameters and the thermodynamic variables can be found in Grenzheuser (12) and Gmehling *et al.* (7).

Methods of Calculation

The problem of phase stability and the calculation of phase equilibrium concentrations have been elegantly attacked in two papers by Michelsen (13, 14). Based on a theorem proved by Baker *et al.* (15) that phase stability requires that at a prescribed T and P the tangent hyperplane to the gibbs energy surface at no point lies above the surface, Michelsen developed methods for first testing a phase for stability, and then estimating an initial concentration guess for calculating phase splits for unstable phases. The method is general and can be used for multiphase equilibria. In a multiphase system, any single phase can be chosen as the test phase. Here we are primarily concerned with V-L and L-L equilibria. Swank and Mullins (16) investigated a number of methods for calculating liquid phase splitting and found that Michelsen's method provided a reliable scheme for the phase split calculations. Their calculations were limited to L-L phase splits using excess free energy models such as UNIQUAC or NRTL (17). Here we are extending use of the method to a complex equation of state. This requires that we carry out conversions from apparent to true mole fractions in each phase under consideration. One useful relation needed for these calculations (see Prausnitz *et al.* (17)) is that the fugacity of a component based on an apparent mole fraction is the same as the fugacity of the monomer based on its true mole fraction.

Prausnitz *et al.* (18) suggest successive substitution as the numerical technique for calculating true mole fractions in a single phase where T, P and the apparent mole fractions are known. Knowing the temperature dependence of the equilibrium constant, K_{ij}, one can write

$$C_{ij} = \frac{z_{ij}}{z_i z_j} = \frac{\hat{\phi}_i \hat{\phi}_j}{\hat{\phi}_{ij}}\, PK_{ij} \tag{17}$$

From initial estimates of the true mole fraction, the dimer true mole fraction is calculated:

$$z_{ij} = C_{ij}\, z_i\, z_j.$$

Grenzheuser (12) has derived the relationship between the apparent mole fraction y_i and the true mole fraction z_i,

$$z_i^{(r+1)} = \frac{y_i \left(1 + \sum_{k=1}^{n} \sum_{j>=k}^{n} C_{kj} z_k^{(r)} z_j^{(r)} \right)}{1 + C_{ii} z_i^{(r)} + \sum_{j=1}^{n} C_{ij} z_j^{(r)}} . \qquad (18)$$

Prausnitz *et al.* (18) suggest a slight twenty percent damping factor be used to assure convergence. Nondimerizing components are included in the normalization of the true mole fractions in each iteration. Initial estimates for the monomer true mole fractions are determined by using the pure component fugacity coefficient and several initial estimate rules (18):

$$C_{ij} = \frac{\phi_i \phi_j}{\phi_{ij}} PK_{ij} \qquad (19)$$

Fitting of Parameters

Gmehling *et al.* (7) and Grenzheuser and Gmehling (3) fitted the pure component parameters to data for liquid volume, vapor volume and vapor pressure for all of the components considered in this work. Figure 7 shows the saturation curve for carbon dioxide; notice the deviation of the data particularly for the vapor volume. In spite of the poor fit for the saturated vapor volume, the saturated vapor pressure is fit well as seen in Figure 8. Predicted values for V-L equilibria in the carbon dioxide-ethane system using a k_{ij} of 0.1002 are shown in Figure 9. Similar calculations indicate that the value of k_{ij} appears to be independent of temperature over a range from 223 to 263 K.

For the ternary systems acetic acid-water-carbon dioxide and acetic acid-water-propane the values of k_{ij} and SO_{ij} are listed in Table III. We chose to use the value of k_{ij} and SO_{ij} for the acetic acid-water as given by Grenzheuser and Gmehling (3). These parameters were fitted to the data of Othmer *et al.* (19) (ΔT = 0.33 K, ΔP = 1.6%, Δy = 1.3 % and appear to be temperature independent (373-530 K, 1-22 bar). The data of Briones *et al.* (1) for carbon dioxide-water (323 K, 68-122 bar) were fitted to yield a value for k_{ij} of 0.0729 which agrees closely with the value of 0.0695 from Grenzheuser and Gmehling (3). Data of Briones *et al.* (1) for the carbon dioxide - acetic acid system (323 K, 56 - 84 bar) when fitted as a function of k_{ij} exhibited a relatively flat objective function in the neighborhood of 0 and a value of –0.01875 was chosen for k_{ij}. The values of k_{ij} fitted to the propane-water data of Kobayashi and Katz (6) showed a temperature dependence, and a value at the temperature of interest was chosen for this work. Since no propane-acetic acid binary data were available, V-L data were calculated using UNIFAC to obtain activity coefficients for the liquid phase and the equation of state of Nothnagel (18) to represent the vapor phase. The calculations were made using ASPEN Plus®. The calculated data were then used to determine a value of k_{ij} for the equation of state used here. The choice of V-L points greatly affects the value of k_{ij}.

Table III. Values of Interaction Parameters Used[a]

Component 1 Component 2	k_{ij} SO_{ij}	T(K) P(Bar)	Reference
Carbon Dioxide Ethane	0.1002	223-263 5-30	Grenzheuser and Gmehling (3)
Carbon Dioxide Water	0.0729	323 68-104	Briones (1)[b]
Carbon Dioxide Acetic Acid	-0.01875	323 56-84	Briones (1)[b]
Propane Water	0.2066	361 6.8-35	Kobayashi (6)[b]
Propane Acetic Acid	0.0592	320 0.1-22	UNIFAC-Nothnagel (Aspen Plus®) generated VLE data
Acetic Acid Water	0.010294 -22.9105	373-505 1-22	Grenzheuser and Gmehling (3)

a - All pure component parameters are from Grenzheuser and Gmehling (3).
b - Data source for fitting k_{ij}

Discussion of Modeling Results

After fitting the required binary parameters, the equation of state was used to predict the ternary systems at the temperatures and pressures for which we have obtained data. The results for the two systems are shown in Figures 3 to 6 and 10 to 12. In these figures the results are plotted as mole fractions on triangular coordinates and also as selectivities and distribution coefficients for acetic acid. As is clearly evident from the results, the predicted values of phase composition along the water-rich side of the ternary are in reasonable agreement with the experimental values, but along the solvent-rich side the agreement is very poor. This result in turn causes the predicted selectivities to be in poor agreement. Experimental densities for the propane-water-acetic acid system compared with the predicted values of the equation of state are shown in Figure 6. The agreement is fair.

The equation of state was not used by Grenzheuser and Gmehling (3) to predict or correlate L-L equilibrium, nor was it used to predict V-L equilibrium in the critical region. However, their parameters were fitted to liquid volumes as well as to vapor volumes and vapor pressures. For this reason we did not refit the pure component parameters in this initial attempt to use the equation to correlate L-L data. Future users of this equation in the critical region should develop a method for refitting the parameters to represent the region more accurately.

SYMBOLS:

A_{nm}	dimensionless constants used to calculate perturbations in the Helmholtz energy (for values see Gmehling *et al.* (7))
c	Prigogine factor
CO_{ij}	parameter of the standard equilibrium constant of dimerization
f	fugacity
Δg°_{R}	standard free energy of reaction
Δh°_{R}	standard enthalpy of reaction
HO_{ij}	parameter of the equilibrium constant of dimerization
k	Boltzmann constant
k_{ij}	binary interaction parameter of the equation of state
K_{ij}	equilibrium constant of dimerization
N_A	Avogadro's number
P	pressure, bar
q	external molecular surface area
r	number of segments in a molecule
R	gas constant
Δs°_{R}	standard state entropy of dimerization
SO_{ij}	parameter of the equilibrium constant of dimerization
T	temperature, Kelvin
T^*	characteristic temperature
$\tilde{T}$	reduced temperature
v	molar volume
v^*	hard-core molar volume
$\tilde{v}$	reduced molar volume`
z	true mole fraction of the different species

GREEK SYMBOLS:

ε	average inter-segment interaction energy
ξ	reduced density
σ	hard-core diameter per segment
ϕ	true fugacity coefficient

SUBSCRIPTS:

i,j,k,l	monomer notation, single species
ij,kl	dimer notation, single species
i	single true species notation
R	reaction

SUPERSCRIPTS:

(r)	iteration number

Acknowledgements

Support of this work from the South Carolina Energy Research and Development Center, Hoechst-Celanese Corporation and the Allied Foundation is gratefully acknowledged.

REFERENCES

1. Briones, J. A., Mullins, J. C., Thies, M. C., and B.-U. Kim, *Fluid Phase Equilib. 36*, 235 (1987).
2. Van Ness, H. C., and M. M. Abbott, *Classical Thermodynamics of Nonelectrolyte Solutions*, McGraw-Hill, New York, NY, 1982.
3. Grenzheuser, P., and J. Gmehling, *Fluid Phase Equilib. 25*, 1 (1986).
4. Goodwin, R. D., *Provisional Thermodynamic Functions of Propane, from 85 to 700 K at Pressures to 700 bar*, National Bureau of Standards, NBSIR 77-860, Washington, DC, 1977.
5. Hartley, I. J., M.S.Thesis, Clemson University, Clemson SC, 1987.
6. Kobayashi, R., and D. L. Katz, *Ind. Eng. Chem. 45*, 440 (1953).
7. Gmehling, J., Liu, D. D., and J. M. Prausnitz, *Chem. Eng. Sci.. 43*, 951 (1979).
8. Donohue, M. D., and J. M. Prausnitz, *AIChE J. 24*, 849 (1978).
9. Carnahan, N. F., and K. E. Starling, *AIChE J. 18*, 1184 (1972).
10. Barker, J. A., and D. Henderson, *Ann. Rev. Phys. Chem. 23*, 489 (1972).
11. Donohue, M. D., Dissertation, University of California, Berkeley, 1977.
12. Grenzheuser, P., Dissertation, Dortmund, Fed. Rep. Ger., 1984.
13. Michelsen, M. L. *Fluid Phase Equilib. 9*, 1 (1982).
14. Michelsen, M. L. *Fluid Phase Equilib. 9*, 21 (1982).
15. Baker, L. E., Pierce, A. C., and K. D. Luks, *Soc. Pet. Eng. J.* 731 (1982).
16. Swank, D. J., and J. C. Mullins, *Fluid Phase Equilib. 30*, 101 (1986).
17. Prausnitz, J. M., Lichtenthaler, R. N., and E. G. de Azevedo, *Molecular Thermodynamics of Fluid-Phase Equilibria*, Prentice-Hall, Englewood Cliffs, NJ, 2nd Ed., 1986.
18. Prausnitz, J. M., Anderson, T. F., Grens, E. A., Eckert, C. A., Hsieh, R., and J. P. O'Connell, *Computer Calculations for Multicomponent Vapor–Liquid and Liquid–Liquid Equilibria*, Prentice-Hall, Englewood Cliffs, NJ, 2nd Ed., 1980.
19. Othmer, D. F., Silvis, S. J., and A. Spiel, *Ind. Eng. Chem. 44*, 1864 (1952).
20. Fredenslund, Aa., and J. Mollerup, *J. Chem. Soc. Faraday Trans. 70*, 1653 (1974).